PORE-FORMING ACTIVITY OF PESTIVIRUS p7 IN A MINIMAL MODEL

SYSTEM SUPPORTS GENUS-SPECIFIC VIROPORIN FUNCTION

Eneko Largo[a], Douglas P. Gladue[b], Nerea Huarte[a], Manuel V. Borca[b], and José L. Nieva[a]

[a]Biophysics Unit (CSIC-UPV/EHU) and Biochemistry and Molecular Biology Department, University of the Basque Country (UPV/EHU), P.O. Box 644, 48080 Bilbao, Spain.

[b]Plum Island Animal Disease Center, ARS, USDA, Greenport, NY 11944, USA.

Corresponding author: José L. Nieva. Biophysics Unit (CSIC-UPV/EHU) and Biochemistry and Molecular Biology Department, University of the Basque Country, P.O. Box 644, 48080 Bilbao, Spain. Phone: +34 94 6013353/ Fax: +34 94 6013360 E-mail: gbpniesj@lg.ehu.es.

Abstract:

Viroporins are small integral membrane proteins functional in viral assembly and egress by promoting permeabilization. Blocking of viroporin function therefore constitutes a target for antiviral development. Classical swine fever virus (CSFV) protein p7 has been recently regarded as a class II viroporin. Here, we sought to establish the determinants of the CSFV p7 permeabilizing activity in a minimal model system. Assessment of an overlapping peptide library mapped the porating domain to the C-terminal hydrophobic stretch (residues 39–67). Pore-opening dependence on pH or sensitivity to channel blockers observed for the full protein required the inclusion of a preceding polar sequence (residues 33–38). Effects of lipid composition and structural data further support that the resulting peptide (residues 33–67), may comprise a bona fide surrogate to assay p7 activity in model membranes. Our observations imply that CSFV p7 relies on genus-specific structures–mechanisms to perform its viroporin function.

Highlights:

- We have established sequence and lipid determinants of CSFV p7 pore formation and its inhibition by channel blockers.
- Analysis with an overlapping peptide library maps the pore-forming domain to the C-terminal hydrophobic region.
- Pore-formation dependence on pH and blocking by amantadine or verapamil requires the turn connecting p7 hydrophobic regions.
- Pore-forming activity of a peptide surrogate was optimal in liposomes emulating membranes of the secretory compartments.
- We conclude that determinants of flaviviral p7 viroporin function are genus-specific.

1. Introduction

The Flaviviridae family comprises of positive-strand RNA viruses, classically classified into three genera: Flavivirus, Pestivirus, and Hepacivirus (Lindenbach et al., 2007). These genera include highly diverse viruses with increasing relevance as both human and animal pathogens. Pestiviruses and hepaciviruses show a high similarity in genome structure and replication mechanisms, and to a lesser extent similarity to flaviviruses (Lindenbach et al., 2007). All viruses belonging to this family translate their RNA into a single polyprotein precursor, which is subsequently cleaved by a combination of host and viral proteases to render structural and non-structural proteins. Specific to the Pestivirus and Hepacivirus genera is the existence of an α-helix-turn-α-helix integral membrane hairpin that connects the structural proteins encoded in the N-terminal portion of the polyprotein with the C-terminal non-structural proteins. After full proteolytic processing of the precursor, the released product, termed p7 (Fig. 1A), remains associated to membranes as an integral membrane protein of approximately 60–70 amino acids (Harada et al., 2000, Lin et al., 1994).

In the last decade an intense research effort has focused on the p7 protein derived from hepatitis C virus (HCV) (reviewed in Steinmann and Pietschmann 2010). This protein is required for production of infectious viruses, but dispensable for viral entry or RNA replication (Steinmann et al., 2007a, Steinmann and Pietschmann, 2010). Moreover, HCV p7 is a viroporin, whose membrane-permeabilizing activity has been proven essential for viral propagation (Jones et al., 2007, Nieva et al., 2012, Wozniak et al., 2010). Consistent with this idea, several compounds have been shown to block HCV p7 pores and inhibit virus production (Foster et al., 2011, Griffin et al., 2003, Steinmann et al., 2007b).

Similarly to hepaciviruses, p7 plays an essential role in the life cycle of pestiviruses and contributes to their pathogenicity (Gladue et al., 2012, Griffin et al., 2004, Luscombe et al., 2010). It has been argued that the pestivirus p7 constitutes a general model for the HCV p7 viroporin, therefore making it useful in the characterization of anti-HCV compounds (Griffin et al., 2004, Luscombe et al., 2010). Here, we have aimed at establishing the determinants of the pestivirus p7 pore-forming activity in a liposome-based model system. Accordingly, we first sought to establish the minimal CSFV p7 sequence required for a pH-dependent pore-forming activity that could be inhibited by channel blockers. Establishment of a shorter active sequence, more amenable for synthesis and purification than the full-length protein, subsequently allowed determining the lipid dependence of the process, and the structural characterization of the pore-forming domain. Together, our data disclose the determinants of the p7 permeabilizing activity, and suggest a new potential means for isolation of antivirals targeting p7.

2. Materials and Methods

The p7 protein and derived peptides displayed in Table 1 were produced by solid-phase synthesis using Fmoc chemistry as C-terminal carboxamides and purified by HPLC. Phosphatidylcholine (PC), phospahtidylethanolamine (PE), phosphatidylinositol (PI), phosphatidylserine (PS), sphingomyelin (SM), cardiolipin (CL) and cholesterol (Chol) were purchased from Avanti Polar Lipids (Birmingham, AL, USA). Dodecylphosphocholine (DPC) was from Anatrace (Maumee, OH, USA). The 8-aminonaphtalene-1,3,6-trisulfonic acid sodium salt (ANTS) and p-xylenebis(pyridinium)bromide (DPX) were obtained from Molecular Probes (Junction City, OR, USA).

Large unilamellar vesicle (LUV) production, ANTS/DPX leakage assays, lipid monolayer penetration determinations and circular dichroism (CD) measurements, were conducted as previously described (Sanchez-Martinez et al., 2008).

Penetration into lipid monolayers was measured to estimate the capacity of p7 peptides for inserting into membranes that mimic different target organelles. In brief, changes in surface pressure were monitored as a function of time in a fixed-area circular trough (μTrough S system, Kibron, Helsinki) measuring 2 cm in diameter and with a volume of 1 ml. The aqueous phase consisted of 1 ml of 5 mM Hepes, 100 mM NaCl (pH 7.4). Lipids, dissolved in chloroform, were spread over the surface and the desired initial surface pressure ($\pi 0$) was attained by changing the amount of lipid applied to the air–water interface. Peptides were injected into the subphase with a Hamilton microsyringe (Fig. S1).

3. Results

3.1: Membrane permeabilizing activity of the full CSFV p7 protein

Fig. 1A displays the CSFV p7 sequence and the hydrophobicity distribution within. The presence of two mainly hydrophobic regions (residues 1–32 and 41–67), intervened by polar residues (33–40) suggests that p7 can form an integral hairpin in membranes (Monne et al., 1999). Furthermore, consistent with a viroporin-like function, a synthetic p7 protein was capable of establishing permeabilizing pores upon addition to a suspension of liposomes that emulate the endoplasmic reticulum (ER) membrane (Fig. 1B). Underscoring the functional relevance of the process, liposome permeabilization was elicited at low pH, the leakage level increasing from virtually 0% to 70% upon lowering the pH value from 7.4 to 4.0 (Fig. 1B left-hand and central panels). Moreover, the process was inhibited by addition of the generic channel blockers amantadine and

verapamil (Fig. 1B, right-hand panel). Thus, this assay provides a suitable means to establish sequence determinants and lipid dependence of pore formation by p7.

3.2: Pore-forming activity dependence on sequence

A library of overlapping synthetic peptides was produced to map the minimal p7 sequence required for pore formation (Table 1 and Fig 2A). To ensure membrane-spanning capacity, the minimal length of these peptides was primarily set to 20 residues. Then, the actual sequence range was established attending to the presence of polar p7 residues with tendency to form turns in membranes (Monne et al., 1999) (Fig. 2A). Thus, the polar sequences overlapping peptides p7–1/p7–2 and p7–2/p7–3 were 16THTDIE21 and 33MRDEPIKK40, respectively. The sequence overlapping peptides p7–3 and p7–4 was longer (residues 39–55). In this case, p7–4 boundaries were selected to span the hydrophobic C-terminal section of p7. The resulting sequence was long enough to transverse the membrane, although interrupted by the turn-promoting 49MTNNPVK55 polar sequence. Finally, to keep the solubility of the synthetic peptides comparable, a Lys-tag were also added to p7–2 and p7–4 as described (Madan et al., 2007).

We have previously reported mutagenesis results indicating that the conserved polar residues within the connection between the potential CSFV p7 transmembrane domains were required for virus production, but not for RNA replication or polyprotein processing (Gladue et al., 2012). Thus, we added to the analysis p7-C, designed to include the turn-promoting residues and the C-terminal transmembrane domain, and an overlapping p7-N, based on the N-terminal section of the protein (Table 1).

Liposome permeabilization levels induced by the different p7-derived peptides are compared in Fig. 2B. Given the activation at low pH observed for the full-length protein and the potential relevance of such effect (Fig. 1), the peptide-library was assayed at pH 5.0. Addition of p7–4 permeabilized the liposomes efficiently, whereas the rest of the peptides were largely inactive. This observation underpins the C-terminal transmembrane section as the p7 pore-forming domain. Data displayed in this figure further indicates that p7-C was also an effective pore-forming peptide, while p7-N was devoid of activity.

To determine the involvement of the conserved 33MRDEPIKK40 turn in pore-forming activity, we further compared in the liposomal system pore-forming activities of p7-C and p7–4 (Fig. 3). Of note, the latter peptide was devoid of the turn-promoting residues, but bore comparable solubility due to the Lys-tag (Table 1). The p7–4 peptide showed higher pore-forming activity as a function of the peptide dose (panel A, right). However, as compared to p7-C, p7–4 activity was not dependent on pH (panel B) or inhibited by addition of the channel blockers amantadine (panel C) or verapamil (panel D). Inhibition of p7-C activity by the latter compounds was actually observed within the same range of concentrations that blocked pore formation by the full-length protein (Fig. 1).

These data would be consistent with pore-forming activity residing at the C-terminal transmembrane section, and with the N-terminal turn residues playing a role at regulating the process. According to this view, p7-C would recreate more precisely than p7–4 the viroporin activity of the full p7 protein.

3.3: Pore-forming activity dependence on lipid

We used p7-C as a minimal version of the full protein to determine the lipid dependence of pore-forming activity. Data displayed in Fig. 4 compare p7-C insertion

induced permeabilization of membranes that emulate different target organelles. Fig. 4A shows results of p7-C-induced permeabilization of ER-like liposomes upon lowering the pH (left panel), and its insertion into monolayers at pH 5.0 and 7.4 (center and right panels). The lipid monolayer technique provides information at the molecular level on peptide interactions with lipid membranes (for a comprehensive review on this method and its application to peptides see: Maget-Dana 1999). In the penetration experiments, p7 peptide insertion into a monolayer of constant area was monitored by following the increase of surface pressure as a function of time (Fig. S1). Induction of high final pressure values, and/or capacity for increasing the surface pressure of highly compressed monolayers (i.e., insertion at high initial pressure values) is consistent with efficient peptide insertion into membranes.

Kinetic traces in the center panel of Fig. 3A disclosed p7-C capacity for increasing the surface pressure of an ER-like lipid monolayer initially compressed at ca. 20 mN/m ($\pi 0$), the process being more efficient at pH 5.0 than at pH 7.4. The right-hand panel discloses the critical pressures (πc-s) for membrane insertion (i.e., the surface pressure at which the peptide was excluded from the lipid monolayer (Fig. S1)). At both pHs, p7-C was capable of penetrating into ER-like monolayers above surface pressures of unstressed natural membranes ($\pi c \geqslant 30$ mN/m, Marsh 2007). However, as compared to pH 5.0 (filled symbols), the lower slope observed at pH 7.4 (empty symbols) for the increase in pressure as a function of $\pi 0$, suggests that reduced amounts of peptide associated with the monolayer under this condition.

The analogous HCV p7 protein has been localized primarily to the ER, but also to the plasma membrane and mitochondria (Carrere-Kremer et al., 2002, Griffin et al., 2005,

Griffin et al., 2004, Haqshenas et al., 2007), which has led the proposal that the p7 product may modify the functions of distinct organelles (Steinmann and Pietschmann, 2010). Thus, we next analyzed the dependence of p7-C pore-forming activity and insertion on the composition of additional target membranes (Table 2). Data displayed in Fig. 4B-top confirmed a pH-dependent permeabilization of membranes emulating the Golgi compartment, but not of those emulating the plasma membrane. Membranes emulating mitochondria were also permeabilized after peptide addition, but the pH effect was less pronounced, and an optimum pH of 6.0 was observed. The source and/or relevance of this difference with respect to the Golgi-like membranes are presently unknown. The corresponding πc-s (Fig. 4B, bottom) denoted more effective insertion into Golgi or mitochondria membranes at pH 5.0. Notably, the peptide could also insert above 30 mN/m into monolayers made of the plasma membrane lipids at both pH's, i.e., under conditions not leading to pore formation. This observation suggests that pore-formation by p7-C inserted into membranes is dependent on the lipid composition, and optimal in membranes emulating secretory compartments.

3.4: Secondary structure determination

Sequence features and functional results so far suggest that the p7-C peptide may embody a transmembrane helical pore, putatively intervened by a short turn. To test this possibility further, we measured p7-C secondary structure in diverse non-polar media and membrane mimics, and compared it with that adopted by the reverting helix represented by p7-N (Fig. 5A). The structural components of both peptides were obtained after deconvolution of CD spectra using the CDPro software package (Sreerama and Woody, 2000). p7-N and p7-C peptides adopted main α-helical conformations in 50% 1,1,1,3,3,3-hexafluoro-2-propanol (HFIP). In this medium p7-C was slightly more helical than p7-

N, albeit not significantly (top-left). Comparatively higher amounts of p7-C helical conformers were also observed in the presence of SDS micelles (top-right), or when dispersed in the membrane-mimic DPC at neutral pH (bottom-left). However, in DPC at pH 5.0 the fraction of p7-N helices decreased significantly, while β-sheet and non-periodic conformers of this peptide increased. In sharp contrast, a subtle increase of p7-C helical structures could be observed under these conditions. Thus, in the presence of DPC phospholipid and acidic pH, the CD data were compatible with stability of the helical structure adopted by the p7-C sequence, while a certain degree of p7-N disorganization seemed to take place. Nonetheless, turn and unordered structures accounted for approximately 30% of the p7-C conformers in DPC under both conditions, consistent with the predicted turn formation in membranes by residues 33MRDEPIKK40 and 49MTNNPVK55 (Fig. 2A).

Together, the previous CD results are consistent with adoption of a main helical conformation by the C-terminal hydrophobic domain of CSFV p7 in the membrane milieu under conditions of optimal pore-forming activity, while non-periodic structures would contribute significantly more to the conformation adopted by the N-terminal sequence. These data support a model for the CSFV p7 channel in membranes in which the C-terminal bipartite helix forms the actual permeating pore (Fig 5B-left). This pore could be recreated in the liposomal system by p7-C, a peptide devoid of the N-terminal hydrophobic domain (Fig 5B-center). In the absence of the 33MRDEPI38 turn, pores could be efficiently formed by p7–4, but were not dependent on pH or inhibited by amantadine or verapamil (Fig. 5B-right).

4. Discussion

In essence, our findings here and the previous report (Gladue et al., 2012) support similar viroporin activities for the p7 products of the members of the Flaviviridae family. However, despite the fact that hepacivirus and pestivirus p7 proteins share a similar class IIA viroporin architecture in membranes (Nieva et al., 2012), the low sequence similarity (Fig. S1A) and the experimental evidence presented here indicate that determinants of the pore-forming function in both proteins might be different.

Our approach in this work identifies the CSFV p7 C-terminal hydrophobic sequence as a pore-forming bipartite helix (Fig. 2, Fig. 3, Fig. 5). According to our results, this domain inserted into membranes of the secretory pathway would display pore-forming activity in the ER and Golgi (Fig. 4). In addition, boosting of the process at acidic pH supports a putative role in alkalinizing the lumen of the Golgi apparatus, in line with the proposed function for other viroporins (Nieva et al., 2012, Wozniak et al., 2010). Structural and biochemical evidence suggests a comparable overall organization for the HCV p7 protein, consisting of two transmembrane segments connected by a short interhelical loop (Carrere-Kremer et al., 2002, Cook et al., 2013, Cook and Opella, 2011, Patargias et al., 2006). However in contrast to our observations, in the hepaciviral p7 protein the N-terminal section has been shown to embody the pore-forming domain (Chew et al., 2009, Montserret et al., 2010, Steinmann and Pietschmann, 2010). Thus, as inferred from computational models (Luik et al., 2009, Patargias et al., 2006, StGelais et al., 2009) and recently reported high-resolution NMR structural data (OuYang et al., 2013), in the prevailing structural model for the HCV p7 pore in lipid bilayers the N-terminal domains form the channel interior, while the reverting chains face the lipid.

Moreover, determinants of amantadine sensitivity seem to be different in both proteins. In the case of HCV p7, mutagenesis identifies a poly-Leu sequence within the reverting C-terminal helix as a main determinant of amantadine sensitivity (StGelais et al., 2009). Consistent with this observation, the binding site has been recently mapped to a hydrophobic pocket between the pore-forming and reverting helices (OuYang et al., 2013). Thus, our finding that the connecting turn determines sensitivity to amantadine in the absence of the reverting helix (Fig. 3) suggests that membrane pores are formed and regulated by different structures–mechanisms in the case of the CSFV p7.

Consistently with the pore-forming activity, the CD results sustain the stability of the p7-C helical conformation in a membrane milieu at low pH, while the conformation adopted by the preceding N-terminal sequence included a majority of flexible conformers (Fig. 5A). Thus, the organization inferred for CSFV-p7 (S2B-left) is opposite to the organization postulated for the analogous HCV p7 inserted into membranes, which consists of a predominantly helical domain at the N-terminus, and a (short)helix-loop motif at the C-terminus (Montserret et al., 2010, OuYang et al., 2013) (Fig. S2 B-right).

Finally our data has implications for the development of antivirals targeting the flavivirus p7 viroporin function. As previously suggested for HCV p7 (Gervais et al., 2011, StGelais et al., 2007), reconstitution of CSFV p7 viroporin function in a liposomal system may be useful for identifying and characterizing new potential antiviral compounds. However, the poor yield of synthesis, owing to the length and hydrophobicity of the sequence, restricts the potential application of the complete protein to systematic experimentation. It has been argued that peptides representing a single transmembrane domain may retain the capacity to assemble ion channels and pores in membranes, and often comprise bona fide surrogates of the full protein sequences (Shai,

1995). Our identification of a shorter version of CSFV p7, more amenable to synthesis, but otherwise retaining its pH-dependent pore-forming activity in a liposomal system, may help in establishing the methodological basis for future antiviral high-throughput screenings.

Overall our observations also imply the existence of essentially different determinants of pore-forming activity in hepaciviruses and pestiviruses. Thus, our experimental data support common inhibition of viroporin function by generic channel blockers such as adamantane or verapamil, but cautions that development of more specific (and likely more potent) inhibitory ligands requires the use of genus-specific sequences-structures.

5. Acknowledgements

6. References:

Carrere-Kremer, S., Montpellier-Pala, C., Cocquerel, L., Wychowski, C., Penin, F., Dubuisson, J., 2002. Subcellular localization and topology of the p7 polypeptide of hepatitis C virus. J Virol 76, 3720-3730.

Chew, C.F., Vijayan, R., Chang, J., Zitzmann, N., Biggin, P.C., 2009. Determination of pore-lining residues in the hepatitis C virus p7 protein. Biophys J 96, L10-12.

Foster, T.L., Verow, M., Wozniak, A.L., Bentham, M.J., Thompson, J., Atkins, E., Weinman, S.A., Fishwick, C., Foster, R., Harris, M., Griffin, S., 2011. Resistance mutations define specific antiviral effects for inhibitors of the hepatitis C virus p7 ion channel. Hepatology 54, 79-90.

Gladue, D.P., Holinka, L.G., Largo, E., Fernandez Sainz, I., Carrillo, C., O'Donnell, V., Baker-Branstetter, R., Lu, Z., Ambroggio, X., Risatti, G.R., Nieva, J.L., Borca, M.V., 2012. Classical swine fever virus p7 protein is a viroporin involved in virulence in swine. J Virol 86, 6778-6791.

Griffin, S., Clarke, D., McCormick, C., Rowlands, D., Harris, M., 2005. Signal peptide cleavage and internal targeting signals direct the hepatitis C virus p7 protein to distinct intracellular membranes. J Virol 79, 15525-15536.

Griffin, S.D., Beales, L.P., Clarke, D.S., Worsfold, O., Evans, S.D., Jaeger, J., Harris, M.P., Rowlands, D.J., 2003. The p7 protein of hepatitis C virus forms an ion channel that is blocked by the antiviral drug, Amantadine. FEBS Lett 535, 34-38.

Griffin, S.D., Harvey, R., Clarke, D.S., Barclay, W.S., Harris, M., Rowlands, D.J., 2004. A conserved basic loop in hepatitis C virus p7 protein is required for amantadine-sensitive ion channel activity in mammalian cells but is dispensable for localization to mitochondria. J Gen Virol 85, 451-461.

Haqshenas, G., Mackenzie, J.M., Dong, X., Gowans, E.J., 2007. Hepatitis C virus p7 protein is localized in the endoplasmic reticulum when it is encoded by a replication-competent genome. J Gen Virol 88, 134-142.

Harada, T., Tautz, N., Thiel, H.J., 2000. E2-p7 region of the bovine viral diarrhea virus polyprotein: processing and functional studies. J Virol 74, 9498-9506.

Jones, C.T., Murray, C.L., Eastman, D.K., Tassello, J., Rice, C.M., 2007. Hepatitis C virus p7 and NS2 proteins are essential for production of infectious virus. J Virol 81, 8374-8383.

Larkin, M.A., Blackshields, G., Brown, N.P., Chenna, R., McGettigan, P.A., McWilliam, H., Valentin, F., Wallace, I.M., Wilm, A., Lopez, R., Thompson, J.D., Gibson, T.J., Higgins, D.G., 2007. Clustal W and Clustal X version 2.0. Bioinformatics 23, 2947-2948.

Lin, C., Lindenbach, B.D., Pragai, B.M., McCourt, D.W., Rice, C.M., 1994. Processing in the hepatitis C virus E2-NS2 region: identification of p7 and two distinct E2-specific products with different C termini. J Virol 68, 5063-5073.

Lindenbach, B.D., Thiel, H.-J., Rice, C.M., 2007. Flaviviridae: The Viruses and Their Replication, in: Knipe, D.M., Howley, P.M. (Eds.), Fields Virology, 5th ed. Lippincott Williams & Wilkins, Philadelphia, pp. 1102-1152.

Luscombe, C.A., Huang, Z., Murray, M.G., Miller, M., Wilkinson, J., Ewart, G.D., 2010. A novel Hepatitis C virus p7 ion channel inhibitor, BIT225, inhibits bovine viral diarrhea virus in vitro and shows synergism with recombinant interferon-alpha-2b and nucleoside analogues. Antiviral Res 86, 144-153.

Madan, V., Sanchez-Martinez, S., Vedovato, N., Rispoli, G., Carrasco, L., Nieva, J.L., 2007. Plasma membrane-porating domain in poliovirus 2B protein. A short peptide mimics viroporin activity. J Mol Biol 374, 951-964.

Marsh, D., 2007. Lateral pressure profile, spontaneous curvature frustration, and the incorporation and conformation of proteins in membranes. Biophys J 93, 3884-3899.

Monne, M., Nilsson, I., Elofsson, A., von Heijne, G., 1999. Turns in transmembrane helices: determination of the minimal length of a "helical hairpin" and derivation of a fine-grained turn propensity scale. J Mol Biol 293, 807-814.

Montserret, R., Saint, N., Vanbelle, C., Salvay, A.G., Simorre, J.P., Ebel, C., Sapay, N.,

Renisio, J.G., Bockmann, A., Steinmann, E., Pietschmann, T., Dubuisson, J., Chipot, C., Penin, F., 2010. NMR structure and ion channel activity of the p7 protein from hepatitis C virus. J Biol Chem 285, 31446-31461.

Nieva, J.L., Madan, V., Carrasco, L., 2012. Viroporins: structure and biological functions. Nat Rev Microbiol 10, 563-574.

Sanchez-Martinez, S., Huarte, N., Maeso, R., Madan, V., Carrasco, L., Nieva, J.L., 2008. Functional and structural characterization of 2B viroporin membranolytic domains. Biochemistry 47, 10731-10739.

Shai, Y., 1995. Molecular recognition between membrane-spanning polypeptides. Trends Biochem Sci 20, 460-464.

Sreerama, N., Woody, R.W., 2000. Estimation of protein secondary structure from circular dichroism spectra: comparison of CONTIN, SELCON, and CDSSTR methods with an expanded reference set. Anal Biochem 287, 252-260.

Steinmann, E., Penin, F., Kallis, S., Patel, A.H., Bartenschlager, R., Pietschmann, T., 2007a. Hepatitis C virus p7 protein is crucial for assembly and release of infectious virions. Plos Pathogens 3, 962-971.

Steinmann, E., Pietschmann, T., 2010. Hepatitis C Virus P7-A Viroporin Crucial for Virus Assembly and an Emerging Target for Antiviral Therapy. Viruses-Basel 2, 2078-2095.

Steinmann, E., Whitfield, T., Kallis, S., Dwek, R.A., Zitzmann, N., Pietschmann, T., Bartenschlager, R., 2007b. Antiviral effects of amantadine and iminosugar derivatives against hepatitis C virus. Hepatology 46, 330-338.

StGelais, C., Foster, T.L., Verow, M., Atkins, E., Fishwick, C.W., Rowlands, D., Harris, M., Griffin, S., 2009. Determinants of hepatitis C virus p7 ion channel function and drug sensitivity identified in vitro. J Virol 83, 7970-7981.

StGelais, C., Tuthill, T.J., Clarke, D.S., Rowlands, D.J., Harris, M., Griffin, S., 2007. Inhibition of hepatitis C virus p7 membrane channels in a liposome-based assay system. Antiviral Res 76, 48-58.

van Meer, G., Voelker, D.R., Feigenson, G.W., 2008. Membrane lipids: where they are and how they behave. Nat Rev Mol Cell Biol 9, 112-124.

Wozniak, A.L., Griffin, S., Rowlands, D., Harris, M., Yi, M., Lemon, S.M., Weinman, S.A., 2010. Intracellular proton conductance of the hepatitis C virus p7 protein and its contribution to infectious virus production. PLoS Pathog 6, e1001087.

7. Figure legends:

Figure 1: CSFV p7 sequence and pore-forming activity. A) Direct translation of pestivirus ssRNA genome gives rise to a single, large polyprotein, which is processed into individual viral proteins. Membrane-integral p7 originates from processing by the host signal peptidase (Top). The hydropathy plot below CSFV p7 sequence is based on the Eisenberg scale. Plotted values represent means for a sliding window of 11 amino acids. Bars denote average values of normalized turn potentials described by Monné et al. (Monne et al., 1999), calculated within sliding windows of 5 amino acids. B) Membrane permeabilization induced by p7 (ANTS/DPX assay). The protein was injected (indicated by the arrow) into stirring solutions of PC:PE:PI (5:3:2 mole ratio) liposomes at a protein-to-lipid ratio of 1:100 (mol:mol). Leakage of vesicular internal aqueous contents was monitored as a function of time. Lipid concentration was 100 µM. The effect of lowering the pH from 7.4 to 4.0 is illustrated in the left and central panels. In the latter the levels of permeabilization after 200 sec was plotted as a function of the assayed pH values. The right panel shows the effect of adding Amantadine (5 mM) or Verapamil (100 µM) on pore-forming activity (red and blue curves, respectively). The black curve corresponds to the control without inhibitor.

Figure 2: Analysis of membrane-permeabilizing activity in a peptide library. A) p7 amino acid sequence and derived peptide library below. B) Left: kinetics of peptide-induced liposome permeabilization. Peptides were added to vesicles at a peptide-to-lipid ratio of 1:250 (mol:mol) and pH 5.0. Right: Bars correspond to permeabilization levels after incubation of peptides with liposomes for 200 sec. Conditions otherwise as in previous Fig. 1B.

Figure 3: Effect of turn-promoting residues on pore-forming activity. A) Comparison of leakage levels induced by p7-C and p7-4. Left: Leakage of vesicle contents induced as a function of time by p7-C and p7-4 peptides (solid and dotted lines, respectively). The peptide-to-lipid ratio was 1:50 and the lipid concentration 100 μM. Right: lytic activity as a function of p7-C and p7-4 dose (filled and empty symbols, respectively). The plotted values correspond to extents of leakage measured 200 s after peptide addition. B) Dependence of leakage on pH. Percentage increase of the extent of leakage at each pH was calculated with respect to the value obtained at pH 7.4. Peptide was added at a peptide-to-lipid ratio of 1:250 and leakage values determined as in the previous panel. C and D) Inhibition of leakage by Amantadine and Verapamil respectively. Extents of leakage in the presence of increasing amounts of inhibitor were determined 200 s after peptide addition. Conditions otherwise as in panel A. Means ± S.D. of three values are represented in panels A-right, B-D.

Figure 4: Interactions of p7-C peptide with membranes emulating the lipid composition of different cell compartments. A) Interactions with membranes emulating the ER composition (Table 2). Left: membrane permeabilization (ANTS/DPX assay). The peptide was injected (addition time indicated by the arrow) into stirring solutions of liposomes at the pHs indicated in the panel. The lipid and peptide concentrations were 100 and 0.4 μM, respectively. Center: Insertion into lipid monolayers. Surface pressure increase was measured in time upon injection of peptide (indicated by the arrow) in the subphase (final peptide concentration: 0.4 μM). The initial pressure of the monolayer was fixed at ≈20 mN/m, and the pH was 7.4 or 5.0 (dotted and solid lines, respectively). Right: Maximum increase in surface pressure induced by the peptide, measured as a function of the initial surface pressure of the phospholipid monolayers incubated at pH 7.4 or 5.0 (empty and filled symbols, respectively). The dotted lines begin at 30 mN/m. The critical

pressures for insertion (π_c-s) are indicated in the panels. B) Interactions of p7-C with membranes emulating the lipid composition of the Golgi apparatus, plasma membrane and mitochondria (Table 2). Measuring conditions for membrane permeabilization (top) and insertion into lipid monolayers (bottom) as described in the previous panel.

Figure 5: Secondary structure of the CSFV p7 hydrophobic regions and proposed architecture within membranes. A) The structural components were calculated for the CD spectra obtained in different non-polar media and membrane mimics, as indicated in the panels. Means ± SD for the fraction values estimated with CONTIN-LL, CDSSTR and SELCON3 programs are plotted for p7-N (black bars) and p7-C (gray bars) peptides. H, helix; S, strand; T+U, turns + unordered. B) Models for the membrane pores established by the full p7 protein (left), and the peptide surrogates p7-C (center) and p7-4 (right). The model suggests that the turn connecting both hydrophobic domains is the determinant for channel inhibition by Amantadine and Verapamil.

8. Tables and Figures

Table 1: Peptide sequences used in this study.

Name	Sequence[a]	CSFV p7 numbering[a]
P7	LQLGQGEVVLIGNLITHTDIEVVVYFLLLYLV<u>MRDEPIKK</u> WILLLFHAMTNNPVKTITVALLMVSGV	1-67
p7-1	LQLGQGEVVLIGNLITHTDIE	1-21
p7-2	THTDIEVVVYFLLLWLV<u>MRDEPIKK</u>-KK	16-40-KK
p7-3	<u>MRDEPIKK</u>WILLLFHAMTNNPVK	33-55
p7-4	KK-KKWILLLFHAMTNNPVKTITVALLMVSGV	KK-39-67
p7-N	LQLGQGEVVLIGNLITHTDIEVVVYFLLLYLV<u>MRDEPIKK</u>	1-32
p7-C	<u>MRDEPIKK</u>WILLLFHAMTNNPVKTITVALLMVSGV	33-67

a: sequences and numbering based on Brescia strain. Underlined residues
correspond to the polar turn proposed to connect two transmembrane domains.

Table 2: Lipid mixtures used in vesicle and monolayer assays

	PC	PE	PI	PS	SPM	CL	Chol
ER[a]	50	30	20	-	-	-	-
Golgi	50	20	10	-	20	-	-
Plasma Membrane	20	12.5	-	5	12.5	-	50
mitochondria	40	35	10	-	-	15	-

a: Mole percentages based on those reported by van Meer et al. (van Meer et al., 2008).

Fig. 1

A

```
              10        20        30        40        50        60
  LQLGQGEVVLIGNLITHTDIEVVVYFLLLYLVMRDEPIKKWILLLFHAMTNNPVKTITVALLMVSGV
```

p7-1 (1-21)   ───────────
p7-2 (16-40)   ───────────
p7-3 (33-55)   ──────────
p7-4 (39-67)   KK-───────────────
p7-N (1-40)   ──────────────────
p7-C (33-67)   ─────────────────
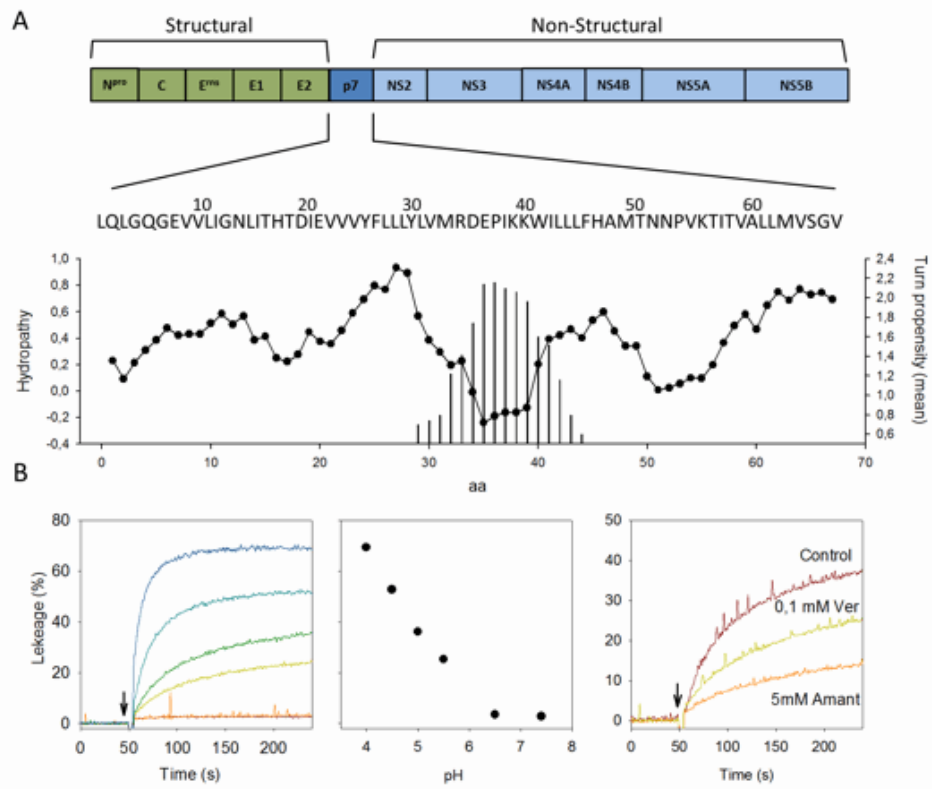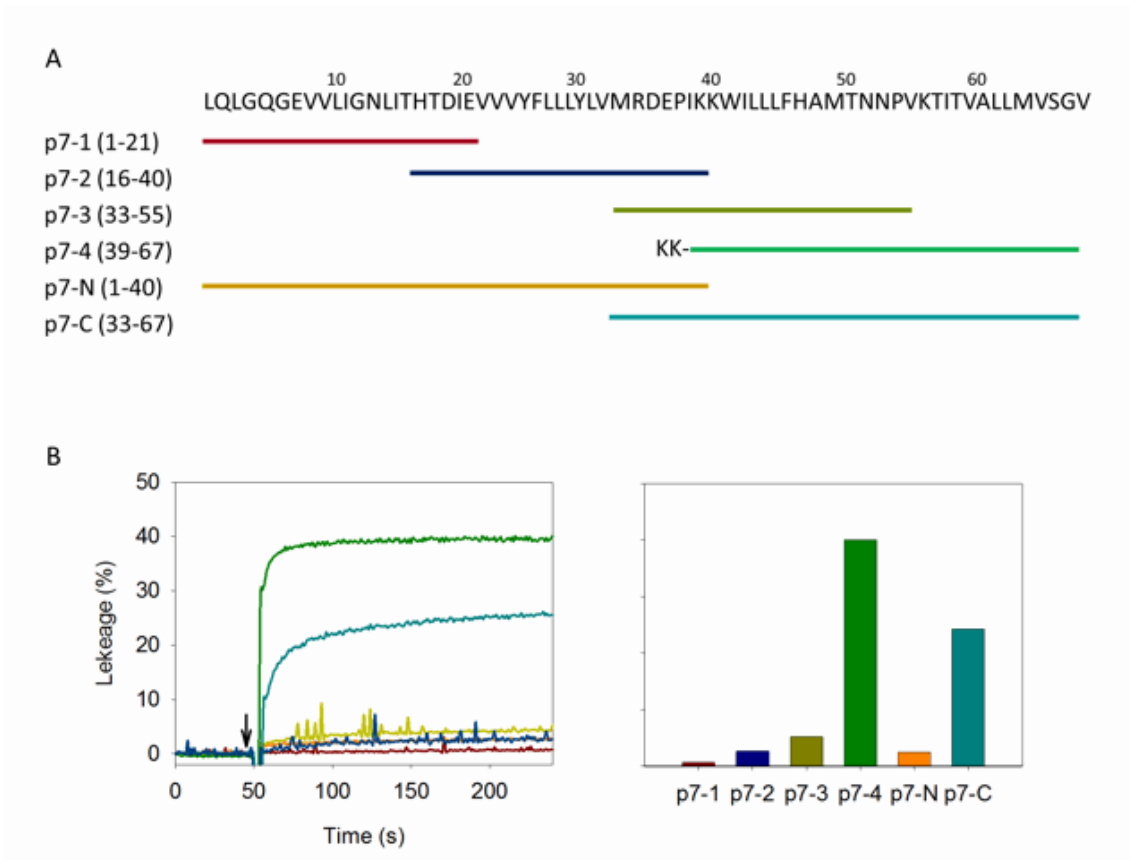
B
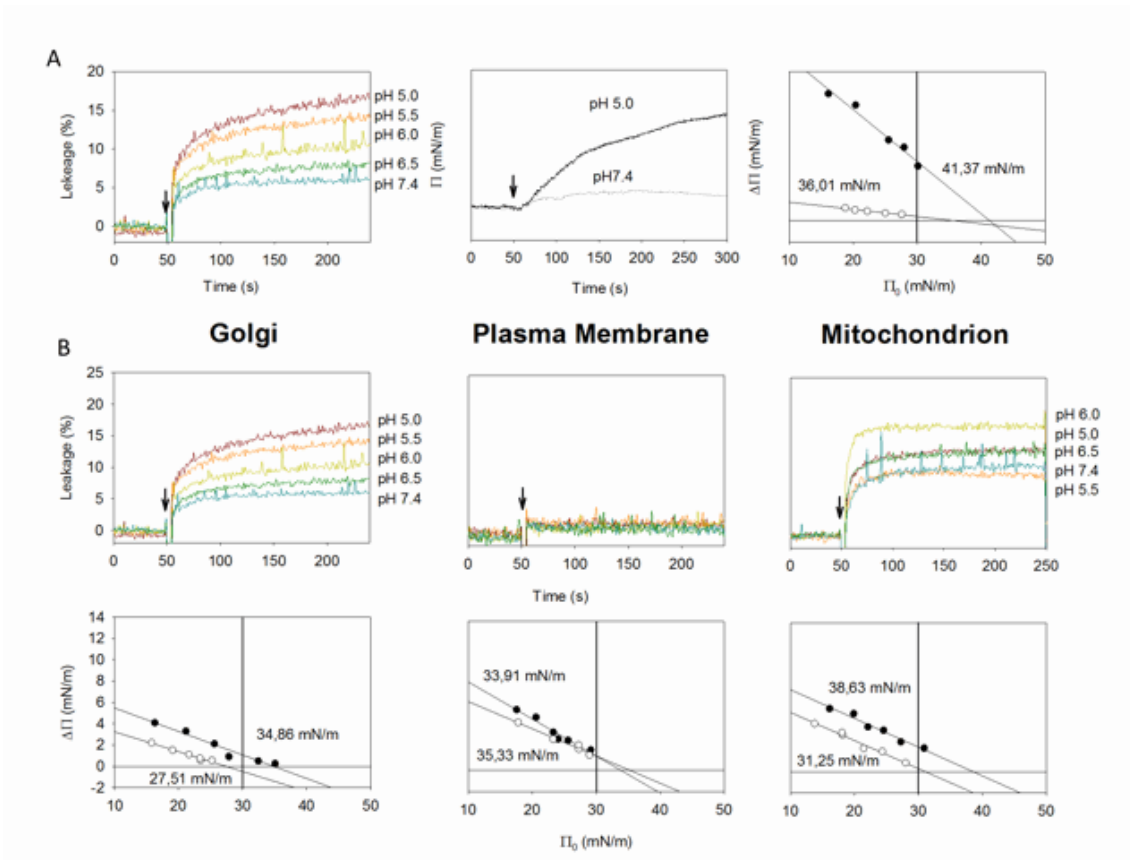

Fig. 2

Fig.3

Fig. 4

26
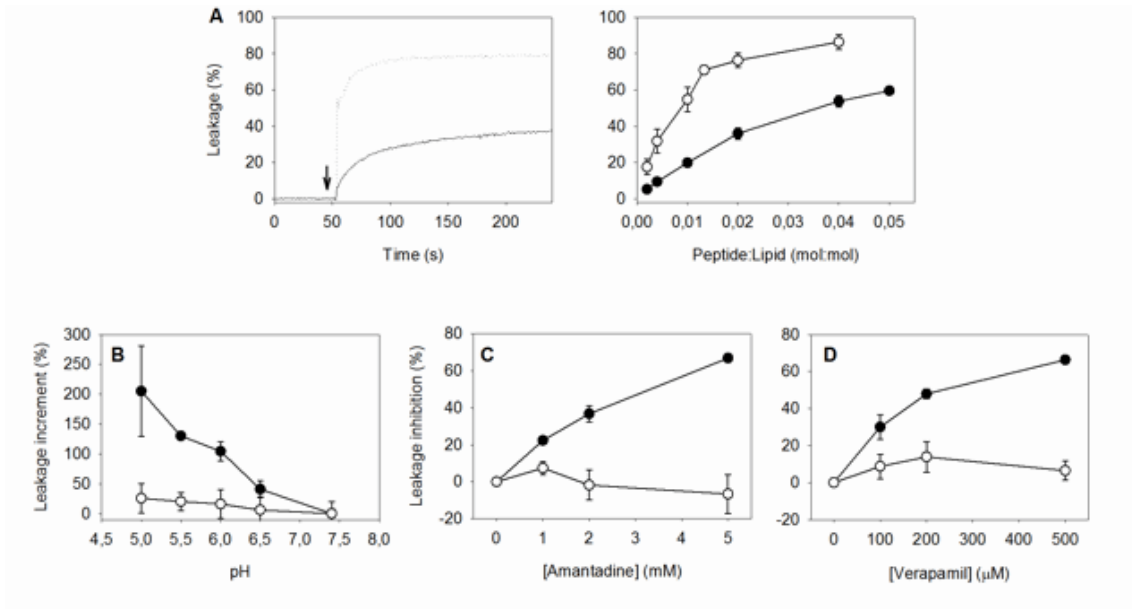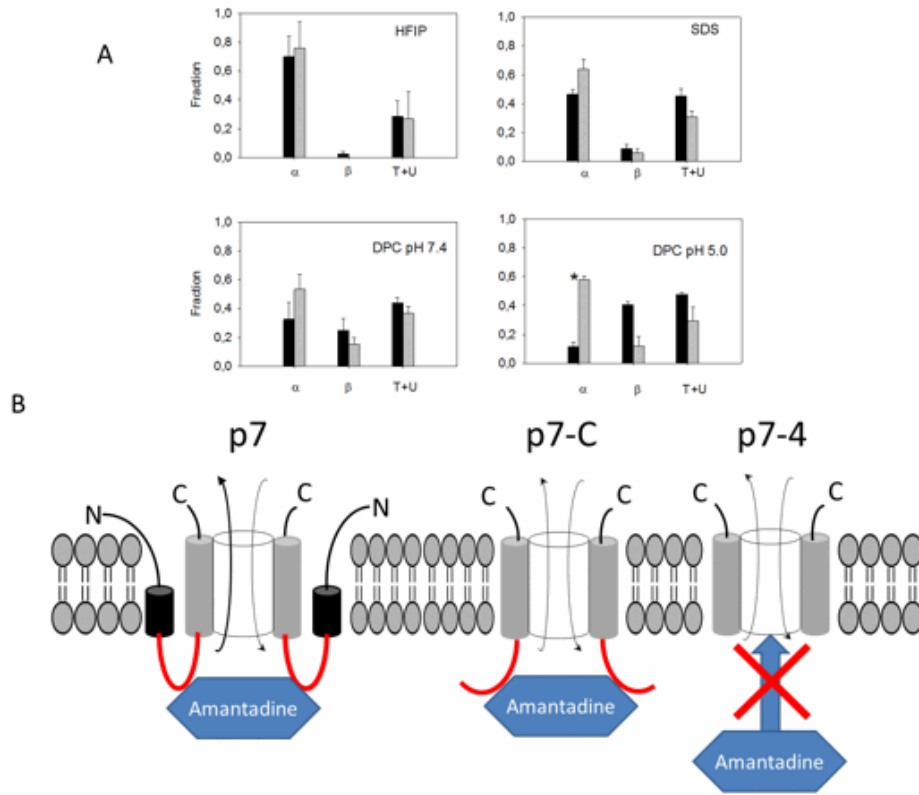
Fig. 5

Supplementary Material:
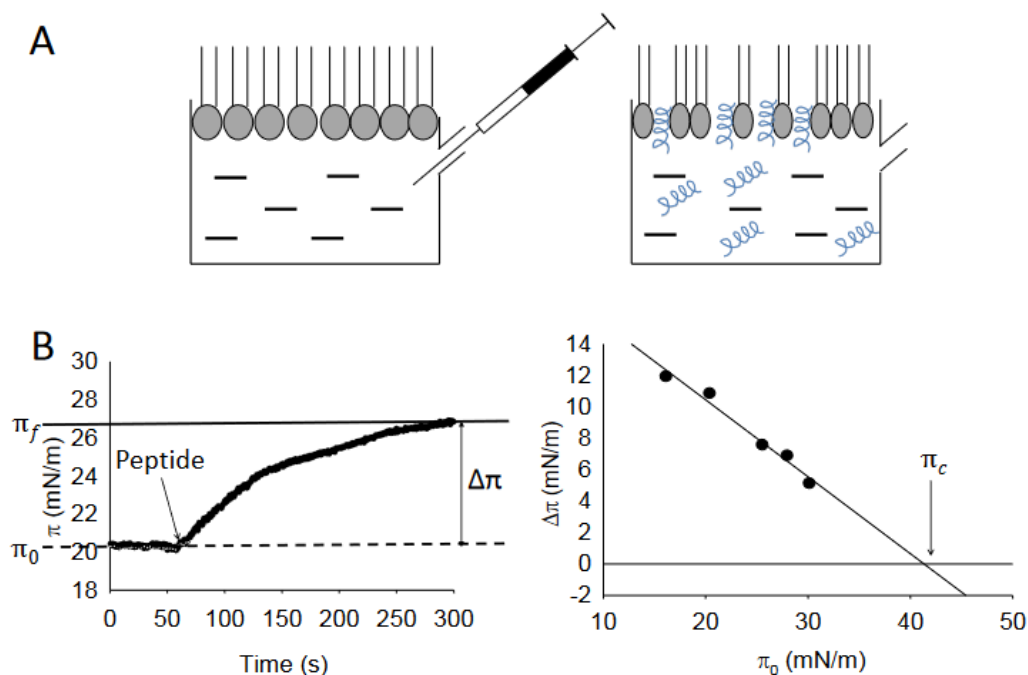
Fig. S1) A) Schematic of the experimental setup used in the lipid monolayer penetration assays. Lipids are spread over the water surface to attain the desired initial surface pressure (left-hand panel). Upon injection into the aqueous subphase, peptide molecules insert into the monolayer thereby increasing its surface pressure (right-hand panel). B) Left: Course of surface pressure kinetics monitored in the Langmuir through. The arrow indicates the peptide addition time. Parameters relevant to our study include: π_0 (initial pressure) and π_f (final pressure), which respectively reflect the initial and final packing of the phospholipids in the monolayer; $\Delta\pi$ (pressure increase), which reflects the packing density increase induced by the peptide upon incorporation into the monolayer. Right: linear regression of $\Delta\pi$ as a function of π_0 values renders the "critical" pressure (π_c) value by extrapolation (the value of x when $y = 0$). This value corresponds to the lipid monolayer pressure at which the peptide no longer penetrates. (Adapted from reference (Maget-Dana, 1999)).

```
A
CSFV Brescia (AAT85717.1)    LQLGQGEVVLIGNLITHTDIEVVVYFLLLYLVMRDEPIKKWIL-LLFHAMTNNPVKTITVALLMVSGV 67
HCV 1ª (CAH23681.1)          -ALEN--LVLLNAASLAGTHGLVSFLVFFCFAWHLK--GKWVPGVAYAVYGMWPLLLLLLALPQRAYA 63
                              *  :  :**:.          :* :::::: :. : :  **:  : : .    *:  : :** :  .

CSFV Brescia (AAT85717.1)    LQLGQGEVVLIGNLITHTDIEVVVYFLLLYLVMRDEPIKKWILLLFHAMTNNPVKTITVALLMVSGV--- 67
BVDV 1 (NP_776265.1)         IQYGSGEVVMMGNLLTHNNIEVVTYFLLLYLLLREESVKKWVLLLYHILVVHPIKSVIVILLMIGDVVKA 70
                             :* *.****::***:**.:****.*******::*:*.:***:***:*  :. :*:*::  *  ***:..*
```

Fig. S2) Comparison of sequences (top) and general architectures in membranes of hepacivirus and pestivirus p7 products (bottom). Alignments on top using HCV, CSFV and BVDV p7 sequences were produced by ClustalW2 (Larkin et al., 2007). The absence of homology (panelA) and the inverse order of the functional domains (panel B) suggest that non-homologous p7 sequences of these genera have functionally converged constrained by their adaptation to permeabilizing membranes of the secretory compartments.

References:

Larkin, M.A., Blackshields, G., Brown, N.P., Chenna, R., McGettigan, P.A., McWilliam, H., Valentin, F., Wallace, I.M., Wilm, A., Lopez, R., Thompson, J.D., Gibson, T.J., Higgins, D.G., 2007. Clustal W and Clustal X version 2.0. Bioinformatics 23, 2947-2948.

Maget-Dana, R., 1999. The monolayer technique: a potent tool for studying the interfacial properties of antimicrobial and membrane-lytic peptides and their interactions with lipid membranes. Biochim Biophys Acta 1462, 109-140.